International Journal of Chemical Science
www.chemicaljournals.com
Online ISSN: 2523-2843
Received: 25-05-2026, Accepted: 24-06-2026, Published: 09-07-2026
Volume 10, Issue 3, 2026, Page No. 7-12

Green fabrication of silver nanoparticles from *Jatropha* leaf extract for metal ion sensing and antibacterial efficacy

Dr. Banoth Reddy[1], Dr. Salluri Udaya Laxmi[2], Dr. M d Moulana Kareem[2], Dr. Hari Babu[3*]
[1] Department of Chemistry, Government Degree College for Women, Khammam, Telangana, India
[2] Department of Chemistry, SR & BGNR Govt. Arts and Science College, Khammam, Telangana, India
[3] NTR. Government Degree College for Women, Mahbubnagar, Telangana, India
Corresponding Author: Dr. Hari Babu
DOI: https://doi.org/10.66856/chemical.2026.10.3.10042

Abstract
This study presents a straightforward, green, and efficient method for synthesizing silver nanoparticles (Ag-NPs) using *Jatropha* leaf aqueous extract used as a reducing agent. The synthesized Ag-NPs displayed a distinct surface plasmon resonance (SPR) peak at 435 nm. Fourier Transform Infrared Spectroscopy (FTIR) analysis identified the functional groups involved in stabilizing and *Jatropha* encapsulating the Ag-NPs. Dynamic Light Scattering (DLS) measurements revealed a particle size distribution of 16 ± 2 nm. Additional characterization was conducted using X-Ray Diffraction (XRD), Scanning Electron Microscopy (SEM), and Transmission Electron Microscopy (TEM). The *Jatropha* encapsulated Ag-NPs exhibited significant antibacterial activity against Escherichia coli and Bacillus subtilis and detection of metal ions.

Keywords: Anti-bacterial, green, leaf extract, ion sensing, silver nanoparticles

Introduction

In recent years, there has been a surge of interest in exploring chemical species at the nanometric scale, fuelled by their immense potential across diverse domains of chemical research [1]. Nanoparticles, with their distinctive amalgamation of size-dependent and metallic properties, have emerged as highly promising candidates for functional applications, capitalizing on their optical, catalytic, and biological attributes [2]. This relevance is particularly pronounced in the contemporary scenario, where the release of substantial quantities of hazardous and non-essential chemicals, gases, and materials into the environment poses significant threats to air and water quality. The quest to unravel nature's mysteries and harness its resources has spurred researchers to devise innovative synthesis methodologies for nanoparticles [3]. Nanotechnology, owing to the unique characteristics of nanoparticles, has demonstrated exceptional suitability for biological applications [4]. Among the plethora of nanomaterials, silver nanoparticles (Ag-NPs) have garnered substantial attention and are extensively utilized in consumer products, as evidenced by numerous studies and reports [5, 6]. Remarkably, over 25% of nano-based products incorporate Ag-NPs, driven by their broad-spectrum biocide activity and cost-effective production [7]. The pervasive adoption of engineered Ag-NPs spans diverse industries, encompassing materials, food, pharmaceuticals, and electronics, as well as drinking water and wastewater treatment applications. Consequently, the release and subsequent accumulation of Ag-NPs in aquatic ecosystems are inevitable [8, 9]. Most environmental modelling studies posit that sewer systems serve as the primary sink for Ag-NPs following discharge from domestic and industrial sources [10].

Jatropha leaf aqueous extract has various biological activities, including antioxidant, anti-inflammatory, antimicrobial, antidiabetic, and anticancer effects, among others [11, 12]. However, its use should be carefully monitored due to potential toxicity, especially when taken in large amounts. *Jatropha* leaf aqueous extract contains a diverse range of phytochemicals, including alkaloids, flavonoids, phenolic compounds, triterpenoids, saponins, and glycosides [13, 14], all of which contribute for the efficient conversion of Ag ions into stable Ag nanoparticles (NPs).

This study was designed to develop an economical, environmentally sustainable, one-step green synthesis approach for producing silver nanoparticles (Ag-NPs) using aqueous extract of *Jatropha* leaves and for metal sensing and antibacterial efficacy.

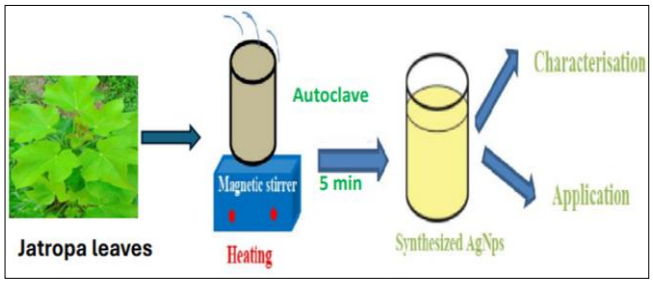

Experimental

Materials and methods

All chemical reagents, including silver nitrate ($AgNO_3$), nitric acid (HNO_3), ferric chloride ($FeCl_3$), zinc chloride ($ZnCl_2$), barium sulfate ($BaSO_4$), sodium chloride (NaCl), magnesium chloride ($MgCl_2$), stannous chloride ($SnCl_2$), copper sulfate ($CuSO_4$), cadmium chloride ($CdCl_2$), nickel chloride ($NiCl_2$), ferrous sulfate ($FeSO_4$), lead nitrate ($Pb(NO_3)_2$), strontium chloride ($SrCl_2$), manganese chloride ($MnCl_2$), potassium chloride (KCl), calcium chloride ($CaCl_2$), and crystal violet dye, were procured from Aura Chemicals. These reagents were of high analytical grade and were utilized without additional purification. Tetley tea powder, renowned for its significant medicinal properties, was sourced from the local market in Hyderabad.

Preparation of *Jatropha* Extract

Jatropha seeds were meticulously ground into a fine powder, and 5 grams of this powder were combined with 100 ml of deionized water. The mixture was then subjected to high-speed centrifugation at 1500 rpm for 30 minutes to effectively separate and remove any insoluble residues. The supernatant was carefully filtered using Whatman filter paper with a pore size of 0.22 microns to yield a clear and purified solution. This filtered extract was subsequently stored under refrigeration at 10°C to preserve its integrity for subsequent applications.

Synthesis of Silver Nanoparticles

A green synthesis approach employing an autoclave process was utilized for the eco-friendly production of silver nanoparticles (Ag-NPs). This method leveraged $AgNO_3$ and *Jatropha* extract, which served dual roles as both reducing and stabilizing agents, eliminating the need for additional external reagents. The synthesis involved combining 1 ml of $AgNO_3$ with 20 ml of *Jatropha* extract, followed by autoclaving at high pressure for 30 minutes [15]. The formation of Ag-NPs was confirmed by a visible color transition from colorless to pale yellow. The synthesized Ag-NPs were subsequently characterized using UV-visible spectroscopy. The process was conducted with varying $AgNO_3$ concentrations (0.1 mM to 0.10 mM) and a fixed *Jatropha* extract concentration (0.5%). The autoclave method provides a rapid, efficient, and sustainable route for nanoparticle synthesis, utilizing pressure and heat to achieve nanoparticle formation in a short duration.

Characterization

To thoroughly elucidate the optical and physicochemical properties of the synthesized Ag-NPs, an array of analytical techniques was employed, encompassing UV-Visible spectroscopy, Fourier Transform Infrared Spectroscopy (FTIR), X-Ray Diffraction (XRD), Scanning Electron Microscopy-Energy Dispersive X-ray spectroscopy (SEM-EDX), Atomic Absorption Spectroscopy (AAS), and Transmission Electron Microscopy (TEM).

Antibacterial Efficacy

The antibacterial efficacy of *Jatropha* encapsulated AgNPs was evaluated against the well and was used to test Gram-positive (B. subtilis) and Gram-negative (E. coli) bacterial strains. Diffusion method. Bacterial inoculum attuned to 0.5 McFarland turbidity norms was spread on Muller-Hinton agar, and wells were created. *Jatropha* capped Ag NPs at various dilutions (1, 5, 10, 50, and 100 µM/mL) were added. After incubation, antibacterial efficacy was assessed by measuring the inhibition zone around each well. Ampicillin served as a reference for comparing the antibacterial efficacy of *Jatropha* encapsulated Ag NPs.

Detection of Metal Ions

In this study, *Jatropha* encapsulated Ag-NPs were used to detect various metal ions (Fe^{2+}, Ba^{2+}, Na^{+}, Mg^{2+}, Sn^{2+}, Cu^{2+}, Ca^{2+}, Al^{3+}, Fe^{3+}, Pb^{2+}, Sr^{2+}, and Mn^{2+}) were prepared and subsequently mixed with 2 ml of the silver nanoparticle solution. The interaction between metal ions and Ag-NPs caused a decrease in UV-Visible absorbance due to the oxidation of Ag-NPs to Ag^{+} ions and the reduction of metal ions. The resulting mixtures were then subjected to UV-Visible spectroscopic analysis.

Results and Discussion

UV-Visible Analysis

The green-synthesized silver nanoparticles (Ag-NPs) produced using *Jatropha* extract through the autoclave method were meticulously characterized using UV-Visible spectroscopy. The synthesized *Jatropha* encapsulated Ag-NPs displayed a distinct surface plasmon resonance (SPR) peak at 435 nm [16], indicative of the formation of spherical nanoparticles with an average size of 16 ± 2 nm (Fig-1), as corroborated by Transmission Electron Microscopy (TEM) and Dynamic Light Scattering (DLS) analyses. The synthesis process involved varying concentrations of silver nitrate ($AgNO_3$), ranging from 0.1 mM to 0.10 mM, each combined with a fixed concentration of *Jatropha* extract (0.5%). UV-Visible spectroscopy revealed a progressive increase in the absorption intensity of the SPR peak with rising $AgNO_3$ concentrations, up to a saturation point [17]. This trend suggests that the quantity of *Jatropha* encapsulated Ag-NPs escalates with higher $AgNO_3$ concentrations while maintaining a consistent proportion of *Jatropha* extract, highlighting the efficiency and controllability of the synthesis process.

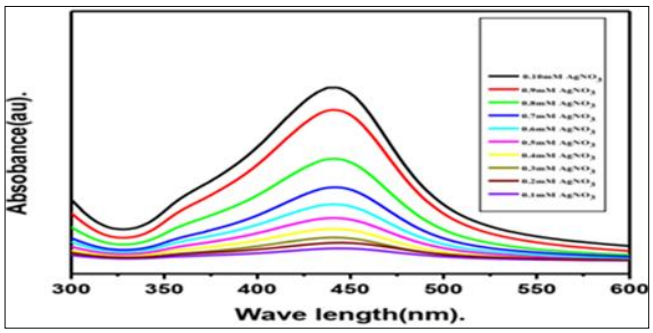

Fig 1: UV spectra of silver nanoparticles (Ag-NPs) synthesized with different concentrations of silver nitrate ($AgNO_3$)

Fourier Transform Infrared Spectroscopy (FTIR)

Fourier Transform Infrared (FTIR) spectroscopy (Fig-2) was utilized to elucidate the phytochemicals involved in the synthesis of silver nanoparticles (Ag-NPs). The FTIR spectrum of *Jatropha* extract exhibited distinct peaks at 1010 cm^{-1}, 1250 cm^{-1}, 1490 cm^{-1}, 1535 cm^{-1}, 1620 cm^{-1}, 2124 cm^{-1}, 2450 cm^{-1}, and 3450 cm^{-1}. A prominent absorption band at 3450 cm^{-1} was identified, corresponding to the stretching vibrations of hydroxyl (-OH) groups. Another notable band at 2450 cm^{-1} was associated with the stretching vibrations of the oxygen-carbon-oxygen (O-C-O) group. Following the reduction of silver nitrate, a decrease in intensity at 1535 cm^{-1} suggested the participation of secondary amines in the reduction process [18]. Additionally, the shift observed at 1620 cm^{-1} was attributed to the interaction of amine and carbonyl groups with the nanoparticles. The presence of functional groups such as (NH), C=O, and O-C-O within the phytochemicals of *Jatropha* extract played a pivotal role in stabilizing the nanoparticles [19]. Specifically, the carbonyl and amine groups were identified as key contributors to the reduction of Ag^{+} ions to Ag nanoparticles. Vibrational groups corresponding to bonds such as C-C (ring), -C-O-C-O-C, and C-C (chain) were derived from water-soluble compounds, including phytochemicals and terpenoids present in *Jatropha* extract, which facilitated the synthesis of silver nanoparticles.

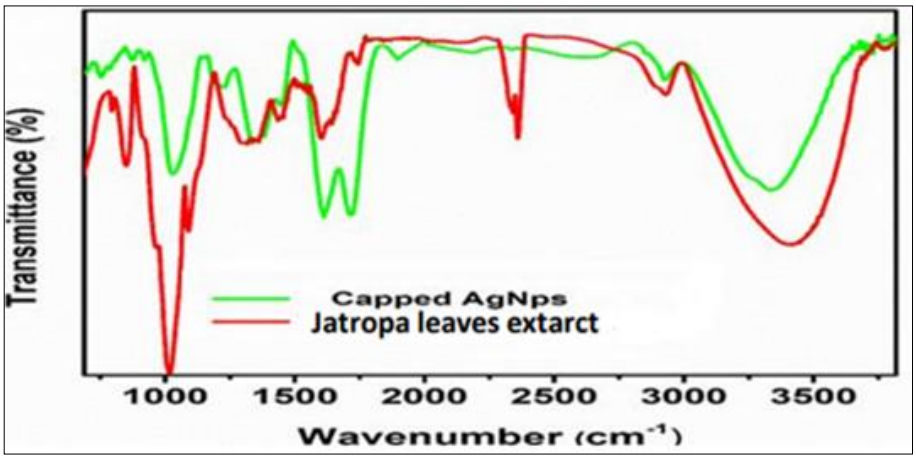

Fig 2: FTIR spectra of Jatropha and Jatropha-capped Ag-NPs

X-Ray Diffraction Studies

X-ray diffraction (XRD) analysis was employed to investigate the crystalline nature, structure, and size of the *Jatropha* encapsulated silver nanoparticles (Ag NPs). The XRD pattern revealed Bragg reflection peaks within the 2Θ range, displaying four distinct and sharp diffraction peaks at 38.24°, 45.34°, 64.9°, and 77.3° in the 20-80° range of 2Θ values (Fig-3). These peaks corresponded to the crystallographic planes (111), (200), (220), and (311), respectively, confirming the formation of *Jatropha* encapsulated Ag NPs with a face-centered cubic (FCC) structure. The observed peak positions closely aligned with the standard JCPDS files 04-0783 and 84-0713 [18].

The average crystalline size (D) of the biogenic Ag NPs, calculated using Debye-Scherrer's equation, was determined to be 18 nm, consistent with the results obtained from Transmission Electron Microscopy (TEM) analysis.

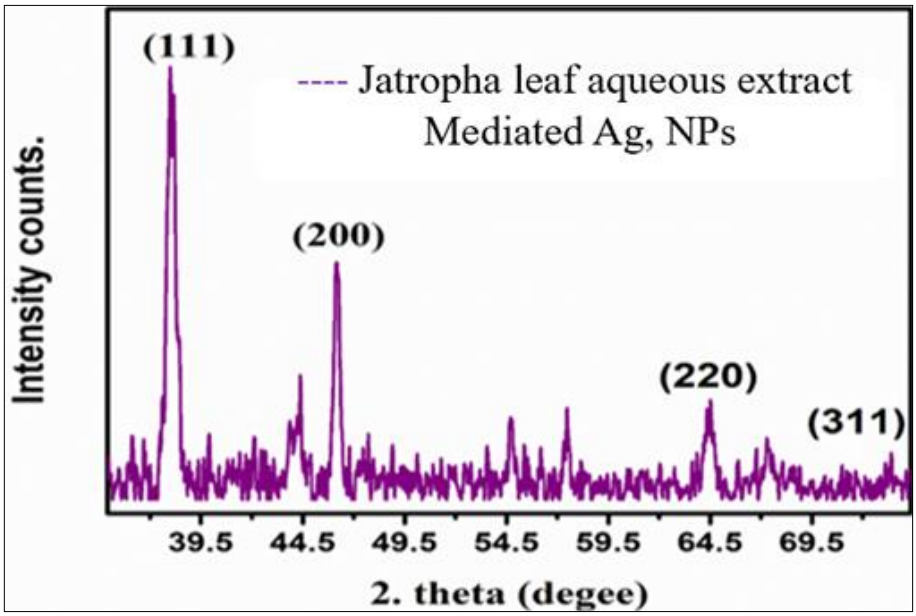

Fig 3: XRD pattern of synthesized Ag-NPs

Scanning Electron Microscope (SEM-EDX)

The characterization of *Jatropha* encapsulated Ag-NPs was carried out using Scanning Electron Microscopy (SEM), a technique that provided detailed insights into the particle size, shape, and distribution by capturing high-resolution micrographs of the *Jatropha* encapsulated Ag-NPs deposited on a film-coated surface (Fig-4a). For SEM sample preparation, the filtrate containing the Ag-NPs was dried under vacuum, and a thin film was prepared by depositing a small aliquot of the sample onto a carbon-coated copper grid. Excess solution was carefully removed using tissue paper, and the film was allowed to dry for 5 minutes under a mercury lamp. SEM analysis revealed the morphology and size of the *Jatropha* encapsulated Ag-NPs, with a particle size distribution of approximately 16 ± 2 nm.

Complementary Energy-Dispersive X-ray (EDX) analysis was conducted to obtain qualitative and quantitative information on the elemental composition of the synthesized *Jatropha* encapsulated Ag-NPs.

The EDX profile confirmed the presence of silver, validating the successful synthesis of the nanoparticles (Fig-4 b). A prominent peak at 3 keV in the EDX spectrum, characteristic of metallic silver nanocrystals, was observed, aligning with the surface plasmon resonance (SPR) typically exhibited by silver nanoparticles [21]. Elemental analysis further indicated a high composition of silver, accompanied by trace amounts of chlorine (Cl) and phosphorus (P), providing additional confirmation of the purity and composition of the synthesized Ag-NPs.

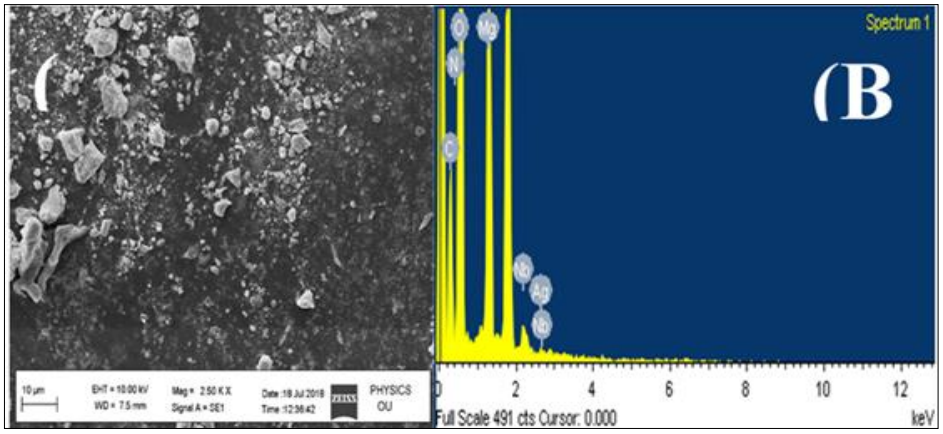

Fig 4: SEM image of (A) Jatropha-capped Ag-NPs and (B) EDX pattern

Transmission Electron Microscope (TEM-DLS)

Transmission Electron Microscopy (TEM) analysis was employed to elucidate the molecular structure and dimensions of the Ag-NPs synthesized using IA extract. The TEM micrographs revealed that the *Jatropha* encapsulated Ag-NPs possess an average size of 16 nm (Fig-5 a-c). Additionally, the analysis indicated that the *Jatropha* extract-capped silver nanoparticles exhibit a spherical morphology with a Face-Centred Cubic (FCC) crystalline structure, corroborated by X-Ray Diffraction (XRD) analysis. The average particle size was determined to be 16 ± 2 nm [22]. The selected area electron diffraction (SAED) pattern featured concentric rings with discontinuous bright spots, further affirming the highly crystalline nature of the nanoparticles (Fig-5 d). These findings align seamlessly with the XRD results, reinforcing the crystalline and structural characteristics of the synthesized *Jatropha* encapsulated Ag-NPs.

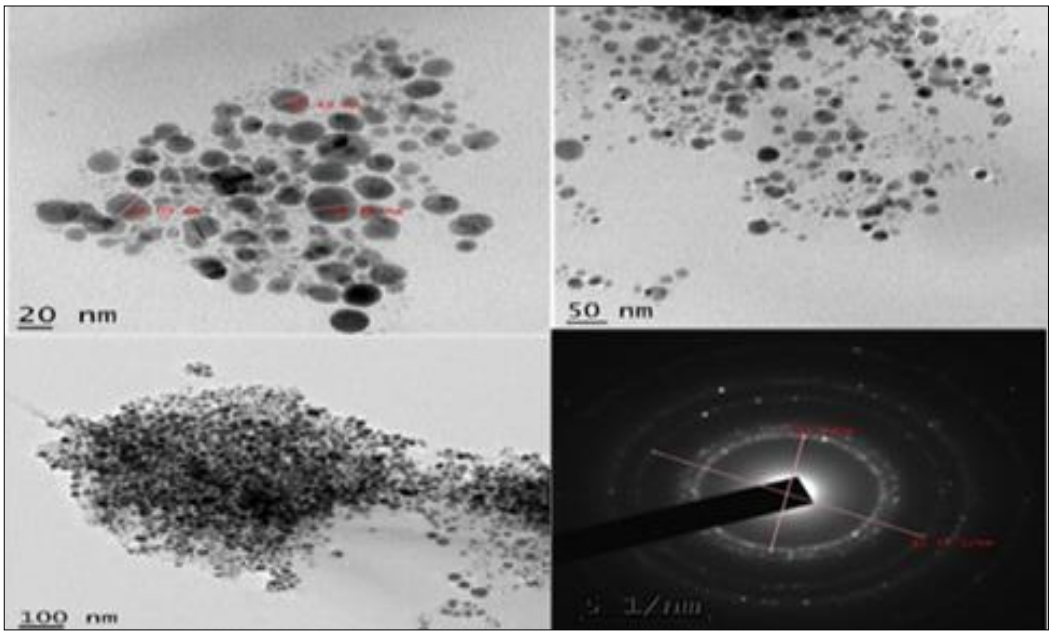

Fig 5: TEM images of (A), (B), and (C) Jatropha-capped Ag-NPs and (D) Selected Area Electron Diffraction (SAED) pattern of silver nanoparticles

Applications

The synthesized *Jatropha* encapsulated silver nanoparticles were strategically employed across a diverse range of applications, encompassing the detection of metal ions, antibacterial efficacy.

Detection of Metal Ions

The detection of metal ions was meticulously conducted using UV-Visible spectroscopy. A series of solutions containing various metal ions (Fe^{2+}, Ba^{2+}, Na^{+}, Mg^{2+}, Sn^{2+}, Cu^{2+}, Ca^{2+}, Al^{3+}, Fe^{3+}, Pb^{2+}, Sr^{2+}, and Mn^{2+}) were prepared and subsequently mixed with 2 ml of the silver nanoparticle solution. The resulting mixtures were then subjected to UV-Visible spectroscopic analysis. Notably, a distinct decolorization of the yellow hue of the silver nanoparticle solution was observed exclusively in the presence of ferric ions (Fe^{3+}), accompanied by a marked reduction in absorbance [23]. This intriguing behavior can be ascribed to the oxidation of *Jatropha* encapsulated silver nanoparticles to silver ions, facilitated by ferric ions, concurrent with the reduction of ferric ions to ferrous ions (Fe^{2+}). This observation underscores the potential utility of silver nanoparticles as a sensitive and selective probe for the detection of Fe^{3+} ions in wastewater or contaminated aqueous environments.

Anti-Bacterial Activity-Interpretation of results

The antibacterial efficacy of *Jatropha* extract-mediated *Jatropha* encapsulated silver nanoparticles (J. Ag NPs) was systematically assessed against two distinct bacterial strains:

a. Bacillus subtilis: The zones of inhibition were recorded as 4, 6, 7, 7, and 10 mm.
b. Escherichia coli: The zones of inhibition were measured at 4, 6, 6, 8, and 9 mm.
c. Ampicillin (standard antibiotic): A consistent zone of inhibition of 4 mm was observed.

The findings revealed that the *Jatropha* encapsulated Ag NPs exhibited significant antibacterial activity against both Bacillus subtilis and Escherichia coli. Notably, the antibacterial potency of the *Jatropha* encapsulated Ag NPs was more pronounced against the Gram-positive bacterium Bacillus subtilis compared to the Gram-negative bacterium Escherichia coli (Table-1). Furthermore, the zones of inhibition for both bacterial strains consistently surpassed those of Ampicillin, underscoring the superior antibacterial performance of the Ag NPs [24, 25]. This suggests that *Jatropha*-mediated Ag NPs hold considerable promise as an effective antimicrobial agent, potentially outperforming conventional antibiotics in specific applications.

Table 1: Antibacterial efficacy of Jatropha-capped Ag-NPs against *Bacillus subtilis* and *Escherichia coli*

S. No.	Name of the Samples	Bacillus subtilis Gram (+ve) Sample Loaded (µl)	Zone of Inhibition (mm)	E. coli Gram (−ve) Sample Loaded (µl)	Zone of Inhibition (mm)
1	0.1 mM $AgNO_3$	60	4	60	4
2	0.2 mM $AgNO_3$	60	6	60	6
3	0.3 mM $AgNO_3$	60	7	60	6
4	0.4 mM $AgNO_3$	60	7	60	8
5	0.5 mM $AgNO_3$	60	10	60	9
6	Ampicillin (Standard)	60	4	60	4

Conclusion

This study presents a green, rapid, and cost-effective synthesis of spherical silver nanoparticles (Ag-NPs) using *Jatropha* extract, eliminating the need for external reagents and utilizing waste biomass for safe, scalable production. Characterization via Transmission Electron Microscopy (TEM) revealed an average size of 16 ± 2 nm, while Dynamic Light Scattering (DLS) indicated a zeta potential of -14.6 ± 7 mV, confirming high stability. The Ag-NPs demonstrated selective detection of Fe^{3+} ions, as evidenced by a significant decrease in UV-Visible absorbance due to the oxidation of *Jatropha* encapsulated Ag-NPs to Ag^{+} and the reduction of Fe^{3+} to Fe^{2+}, showcasing their potential for monitoring Fe^{3+} in polluted water. Additionally, the *Jatropha* encapsulated Ag-NPs exhibited superior antibacterial activity against Bacillus subtilis (Gram-positive) compared to Escherichia coli (Gram-negative), with inhibition zones exceeding those of Ampicillin, highlighting their enhanced antibacterial efficacy. These findings underscore the versatility of *Jatropha*-mediated Ag-NPs in environmental and biomedical applications.

Acknowledgments

The authors extend their appreciation to the Department of Chemistry at Osmania University and to CFRDOU for their provision of essential infrastructure.

Conflict of Interests

The authors affirm that there are no conflicts of interest related to the publication of this article.

Author Contributions

Each author made substantial contributions to this manuscript, participated in its review and editing, and endorsed the final draft for publication.

References

1. Yaku G, Rekha KC, Rao TVDP. International Journal on Emerging Technologies,2019:10:325.
2. Kareem MM, Hari Babu M, Vijaya Lakshmi G. Inorganic Chemistry Communications,2023:148:110274.
3. Arumai Selvan D, Mahendiran D, Senthil Kumar R, Rahiman K. Journal of Photochemistry and Photobiology B: Biology,2018:180:243.
4. Qing W, Chen K, Wang Y, Liu X, Lu M. Applied Surface Science,2017:423:1019.
5. Nakhjavani M, Nikkhah V, Sarafraz MM, Shoja S, Sarafraz M. Heat and Mass Transfer/Waerme- Und Stoffuebertragung,2017:53:3201.
6. Rolim WR, Pelegrino MT, de Araújo Lima B, Ferraz LS, Costa FN, Bernardes JS, *et al*. Applied Surface Science,2019:463:66.
7. Haghparasti Z, Mahdavi Shahri M. Materials Science and Engineering C,2018:87:139.
8. Alsammarraie FK, Wang W, Zhou P, Mustapha A, Lin M. Colloids and Surfaces B: Biointerfaces,2018:171:398.
9. Zeb N, Ali J, Bilal M, Omer M, Alamzeb M, Salman SM, *et al*. Ijn-14-5087. Pdf, 2019, 5087.
10. Ren Y, Yu Y, Yang H, Wang T, Wang T, Wang C. Physics Letters, Section A: General, Atomic and Solid State Physics,2016:380:3773.
11. Sökmen M, Alomar SY, Albay C, Serdar G. Journal of Alloys and Compounds,2017:725:190.
12. Shabina S, Gaurav S, Irfan AM, Sarmad M. Research Journal of Biotechnology,2020:15:177.
13. Alfuraydi AA, Devanesan S, Al-Ansari M, AlSalhi MS, Ranjitsingh AJ. Journal of Photochemistry and Photobiology B: Biology,2019:192:83.
14. Girón-Vázquez NG, Gómez-Gutiérrez CM, Soto-Robles CA, Nava O, Lugo-Medina E, Castrejón-Sánchez VH, *et al*. Results in Physics,2019:13:102142.
15. Activities A. Journal of Applicable Chemistry,2014:3:1560.
16. Ahmed S, Saifullah, Ahmad M, Swami BL, Ikram S. Journal of Radiation Research and Applied Sciences,2016:9:1.
17. Roy A, Bulut O, Some S, Mandal AK, Yilmaz MD. RSC Advances,2019:9:2673.
18. Roy S, Das TK. International Journal of Plant Biology,2015:3:1044.
19. Mousavi SM, Hashemi SA, Ghasemi Y, Atapour A, Amani AM, Savar Dashtaki A, *et al*. Artificial Cells, Nanomedicine and Biotechnology,2018:46:S855.
20. Abdelghany TM, Al-Rajhi AMH, Al Abboud MA, Alawlaqi MM, Ganash Magdah A, Helmy EAM, *et al*. BioNanoscience,2018:8:5.
21. Khalil MMH, Ismail EH, El-Baghdady KZ, Mohamed D. Arabian Journal of Chemistry,2014:7:1131.

22. Rauwel P, Kuunal S, Ferdov S, Rauwel E. Advances in Materials Science and Engineering,2015:2015:682749.
23. Manosalva N, Tortella G, Cristina Diez M, Schalchli H, Seabra AB, Durán N, *et al*. World Journal of Microbiology and Biotechnology,2019:35:1.
24. Singhal G, Bhavesh R, Kasariya K, Sharma AR, Singh RP. Journal of Nanoparticle Research,2011:13:2981.
25. Yousaf H, Mehmood A, Ahmad KS, Raffi M. Materials Science and Engineering C,2020:112:110901.
26. Seerangaraj V, Sathiyavimal S, Shankar SN, Nandagopal JGT, Balashanmugam P, Al-Misned FA, *et al*. Journal of Environmental Chemical Engineering,2021:9:105088.
27. Choleva TG, Tsogas GZ, Giokas DL. Talanta,2019:196:255.